Materials Research Proceedings 38 (2023) 120-130 https://doi.org/10.21741/9781644902837-18

Simulation-Based Manufacturing of Near-Net-Shape Components and Prediction of the Microstructural Evolution during Hot Isostatic Pressing

Yuanbin Deng[1,a *], Anke Kaletsch[1,b] and Christoph Broeckmann[1,c]

[1] RWTH Aachen University, Institute for Materials Applications in Mechanical Engineering, Augustinerbach 4, 52062, Aachen, Germany

[a]y.deng@iwm.rwth-aachen.de, [b]a.kaletsch@iwm.rwth-aachen.de, [c]c.broeckmann@iwm.rwth-aachen.de

Keywords: Hot Isostatic Pressing (HIP), Discrete-Element-Method (DEM), Capsule Filling, Finite-Element-Method (FEM), Densification, Phase Transformation/precipitation, Modelling, Simulation

Abstract. Following the development of hot isostatic pressing (HIP) with integrated rapid cooling technology, it is now possible to combine consolidation of encapsulated powder and subsequent heat treatment in a single step. In this study, the influences of pressure and cooling rate on the microstructural evolution of martensitic and duplex steels during the entire HIP process with rapid cooling are investigated. Besides the microscopic investigation of the microstructure, a material model for finite element (FE-) simulations was developed to numerically correlate the understanding based on experiments and to predict the final shape of the HIP component. This FE-simulation was additionally employed in the capsule design to achieve net-shape production of the components with complex geometries. The agreement between the experimental and simulated results validated the method to be able to ensure a near-net-shape product and to monitor microstructural development during HIP and rapid cooling.

Introduction

Hot isostatic pressing (HIP) is widely applied in powder metallurgy (PM) to produce components with high requirements on the final geometry and properties, as it densifies metal powder to a fully dense bulk component with a homogeneous, isotropic, and fine-grained microstructure [1]. The Powder HIP involves filling of metal powder into a metallic capsule and consolidating of the powder to full density in a HIP unit. Due to the limited filling density of the powder after pre-densification, the capsule shrinks up to about 30% in volume during the HIP process. Thereafter, the capsule has either reached its net-shape geometry or has to be further processed as a semi-finished product. Conventional capsules for powder HIP are welded from sheet metal and thus are restricted to produce components with simple geometries. With the development of additive manufacturing (AM), it is possible to build predestined complex-shaped HIP capsules, thus, the net-shape parts can also be achieved by using optimized capsule geometry with the help of numerical simulation [2]. Besides near-net-shape manufacturing, the adjustment of the microstructure of the final component in order to achieve desired mechanical properties remains challenging. Based on the increasing attraction of applying HIP with integrated rapid cooling to produce materials like martensitic and duplex stainless steels, where specific microstructural constituents significantly determine the properties of the component, a further development of the macroscopic HIP models is required to predict the evolution of the microstructure. To realize this, the understanding of the kinetics of the studied microstructural constituents as well as the heat transfer between the cooling gas and the component in the HIP unit are indispensable. The former provides sufficient parameters that can be implemented in the simulation model. The latter offers

Materials Research Proceedings 38 (2023) 120-130 https://doi.org/10.21741/9781644902837-18

an accurate description of the temperature distribution in the component. As a result, the evolution and distribution of phases within the whole component can be accurately predicted during cooling. This work focuses on the simulation-based manufacturing of near-net-shape components with the prediction of the microstructural evolution during hot isostatic pressing. Capsule filling, near-net-shape manufacturing and the prediction of microstructural constituents has been studied by an extruder screw as an example for a typical component. The additively produced capsule of AISI A11 was filled with AISI L6 powder. The phase transformation during the cooling stage was modelled and numerical studied. By employing a second demonstration component that is made of AISI 318LN, filled in a conventionally produced capsule, a precipitation model was developed, which allows the prediction of σ−phase volume fraction with the consideration of heat transfer analysis during HIP with integrated rapid cooling. The numerical methods developed here are expected to support powder HIP of near-net-shape components with complex geometries and desired microstructure by adjusting the capsule design.

Materials and modelling

Materials, capsule geometries and HIP cycles

In this work, the capsules with two different geometries (Fig. 1 (a) and (b)) were hot isostatically pressed using the integrated rapid cooling option. These capsules (a) and (b) were made of two different kinds of steels and filled with two different powders, respectively, as listed in Table 1. The HIP cycles for both capsules had a heating rate of 500 K/h, a holding temperature of 1150°C, and a pressure of 100 MPa. The holding times for capsules/powder AISI A11/AISI L6 and AISI 304/AISI 318LN were 3 h and 2 h, respectively. To determine the model parameters and to manufacture near-net-shape components, several HIP-units were used in this work, which are listed in Table 2. All capsules were cooled down rapidly in the HIP vessel subsequent to the holding stage.

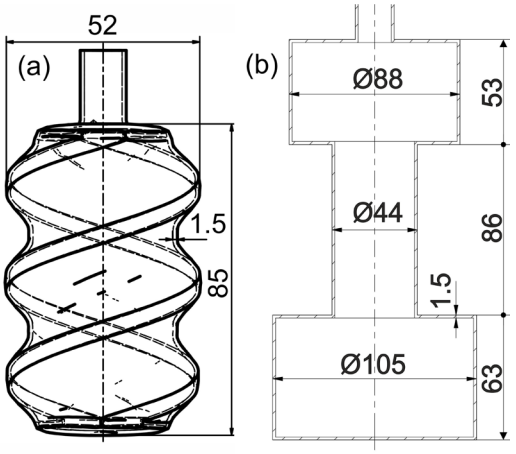

Figure 1: Capsule geometries

Table 1: Applied materials of capsules (a) and (b) during HIP.

Capsule geometry	Capsule	Powder/Bulk
(a)	Martensitic tool steel AISI A11 (FeCrV10)	Martensitic tool steel AISI L6 (DIN 56NiCrMoV7)
(b)	Stainless steel AISI 304 (DIN X5CrNi18-10)	Duplex stainless steel AISI 318LN (DIN X2CrNiMoN22-5-3))

Table 2: HIP units and types.

Capsule	HIP unit, type	Integrated rapid cooling unit
(a)	QIH-15L Quintus Technologies, Sweden	√
(b) and cycles for the determination of model parameters	QIH-9, Quintus Technologies, Sweden	√
	Shirp 20/30-200-1500, ABRA Fluid AG, Switzerland and reconstructed by Cremer Thermoprozessanlagen GmbH	√

Materials Research Proceedings 38 (2023) 120-130 https://doi.org/10.21741/9781644902837-18

Modelling of particle flow and capsule filling

Since the powder filling process can be seen as a granular system and each particle in this system moves independently, it is difficult to predict the behavior of the granular system using continuum mechanical models. In this context, the discrete approach developed for numerical modelling of granular materials at particle scale, which is generally referred to as discrete element method (DEM) [3, 4], has become a powerful and reliable tool. DEM is a particle method based on Newton's laws of motion. In this method, particles are defined as soft particles that can move with six degrees of freedom (three for translational and three for rotational movements), but only undergo elastic deformation. In this way, the simulation of the contact between particles considers a cohesive force (F_{ij}^{Coh} in Eq. (1)), which is calculated by a contact model and a cohesion model. The Hertz–Mindlin model, as a widely used contact model, describes the normal interaction by a nonlinear relationship which represents the elastic contact behavior between particles. When the distance d_{ij} between two particles is smaller than their contact distance $R_i + R_j$, the model is used to calculate the Hertz–Mindlin contact force F_{ij}^{HM}. The simplified model of Johnson-Kendall-Roberts (SJKR) as the cohesion model adds an additional normal force contribution to the Hertz-Mindlin model. If two particles are in contact, the SJKR model adds an additional normal force F_{ij}^{Coh}which helps to maintain the contact. In addition to the contact forces, gravitational acceleration is also considered and the gravitational force F_i^{Grav} is calculated [5]. In this way, all forces on a particle can be calculated as follows:

$$F_{ij}^{sum} = F_{ij}^{HM} + F_{ij}^{Coh} + F_i^{Grav} \tag{1}$$

Newton's equations of motion are used to determine the new positions of the particles. The equations of the interaction forces and moments in a time step for particle i are as follows

$$m_i \ddot{x}_i = F_i^{sum} \tag{2}$$

$$I_i \dot{\omega}_i + \omega_i \times I_i \cdot \omega_i = t_i \tag{3}$$

where m_i is the mass, $\ddot{x}_i$ is the acceleration, I_i is the Inertia tensor, ω_i is the angular velocity, $\dot{\omega}_i$ is the angular acceleration, and force F_i^{sum} and moment t_i are the sums of all forces and moments that act on the particle.

Modelling of densification during hot isostatic pressing

Many mechanisms, which take place during densification of powder in a HIP process such as particle rearrangement, plastic and viscoplastic deformations as well as diffusion, determine the final properties of the produced components. The contribution of each mechanism depends on the processing parameters in the individual HIP stage. Throughout the early stage, the particle rearrangement and the growth of necks at the contact points between the particles dominate the densification following the continuously increasing pressure and temperature. In the following stage, the necks grow until they impinge, and the individual pores are sealed off [6]. The rate-dependent deformation mechanisms overtake the granular dominated material behaviors at elevated temperature and pressure. Among these mechanisms, the two most significant ones that lead to the changes in density and volume are plastic yielding and viscoplastic deformation. Therefore, to precisely describe the material behaviors during HIP, the time independent plasticity model of Kuhn and Downey [7] was coupled with the time dependent plasticity (viscoplasticity) model of Abouaf et al. [8]. Both models have been proven by Wikman et al. [9] to be the best approaches to simulate the densification of porous media under the effect of high isostatic pressure.

In previous publications of the authors [10–12], the constitutive equations and the implementation steps were given in detail.

Modelling of microstructural evolution during continuous cooling

The evolution of the microstructure, residual stresses and deformation during cooling is the outcome of a multi-physics process including different physical fields and the interactions between them. For a quantitative and predictive description in the cooling stage of the HIP cycle, a numerical approach is adopted, which considers the relevant themomechanical-metallurgical coupling. The featured interactions result in a time and position dependent stress/strain state. During quenching, thermal stresses arise due to the temperature gradient between the component's surface and core, which is determined by the heat transfer between the component and the pressurized gas. With the implementation of the experimentally determined heat transfer coefficient in the model, the inhomogeneous temperature distribution in the component that induces a heterogeneous microstructure after cooling is considered in the simulation.

The phase transformations have major contributions to the evolution of the microstructure as well as the geometrical distortion induced deformations and stresses during cooling. Hence, a reasonable description of the microstructural evolution that is important for the simulation of the cooling process requires a reliable modelling of the phase transformation kinetic. In this work, the diffusionless transformation (austenite→ martensite) is modelled by applying a slight modification to the Koistinen Marburger approach [13]. There is no need to formulate the model as a differential equation in this case because the transformation is time independent and thus, the equation (4) is directly implemented for the simulation of the transformation.

$$p_m = \tilde{p}_m \cdot \left[1 - exp\left\{-\left(\frac{M_s(\lambda) - T}{b(\lambda)}\right)^{n(\lambda,T)}\right\}\right] \tag{4}$$

In the equation (4), p_m is the volume fraction of martensite, $\tilde{p}_m$ is the maximum possible fraction of martensite which depends on the available austenite amount, M_s is the martensite start temperature, λ is the cooling parameter, T is the temperature ($T < M_s$), and finally b and n are material specific parameters. The new feature of this model adopted from [13] is that the effect of the cooling parameter on the kinetic of the martensitic transformation is considered. Unlike the martensitic transformation, the diffusion-controlled transformations (austenite →ferrite/perlite/bainite) are modeled using the modified Avrami equation as in [14]. The derivative form of the equation (5) is applied to adapt it to non-isothermal conditions by eliminating the time factor given in the original Avrami-model [14–16].

$$\dot{p} = n(T) \cdot \frac{\tilde{p}(T) - p}{\tau(T)} \cdot \left[ln\left(\frac{\tilde{p}(T)}{\tilde{p}(T) - p}\right)^{\frac{n(T)-1}{n(T)}}\right] \cdot f_1 \cdot f_2 \tag{5}$$

In equation (5), $\dot{p}$ is the rate of the transformation and p is the volume fraction of the newly build phase. The kinetic parameters $n(T)$ and $\tau(T)$ depend on the nucleation and the growth rate. $\tilde{p}(T)$ is the maximum possible volume fraction of the product phase at the given temperature. This kind of formulation allows to consider the effect of different thermomechanical conditions on the kinetic of the transformation. For instance, the effect of the cooling rate on the transformation is modeled by a correction factor $f_1(\dot{T})$. Similarly, a factor f_2 could be applied to represent another interaction such as the effect of plastic deformations or the austenite grain size on the transformation kinetic.

Materials Research Proceedings 38 (2023) 120-130 https://doi.org/10.21741/9781644902837-18

After minor modifications, this modified Avrami model can be further used to describe the phase precipitation during continuous cooling quantitatively [10], considering that the precipitation kinetics of the precipitate phase including nucleation and grain growth are controlled by the thermodynamic driving forces and the diffusion, respectively.

Numerical studies

Capsule filling

The DEM modelling technique was used to simulate the capsule filling. To consider the powder size distribution from the real powder, a simplified and upscaled powder model was created. As the number of particles in a DEM simulation cannot be defined arbitrarily due to the limitation of the computational power, it is not yet possible to simulate any given real system on a one-to-one particle level. To shorten the computational time, a coarse graining strategy was developed in the DEM modelling, which is capable of quantitatively describing static and dynamic behaviors of real powders. The size distribution of the modelled particles was adjusted to represent the experimental values obtained from real powder particles in different size categories (Table 3). To calibrate the scaling factors after grain-coarsening, the DEM model parameters (e.g., coefficient of restitution, friction coefficient, and cohesion energy density) of AISI L6 powder were adjusted in modelled experimental setups until the simulation results agreed with the experimentally measured data.

Table 3: Particle size distribution of real powder and modelled powder particles in four size categories

Particle size distribution of L6 powder					
Real powder		Simplified		Upscaled and modelled via DEM (Scaling factor 2.5)	
Radius [µm]	Weight [%]	Radius [µm]	Weight [%]	Radius [µm]	Weight [%]
0-57	11.80	54	15	135	15
58-99	32.50	84	30	210	30
100-149	38.70	114	35	285	35
150+	17.10	150	20	375	20

Simulation of the filling process with capsule geometry (a) was carried out in the LIGGGHTS software v3.8.0, which is a parallel particle simulator developed by DCS Computing GmbH, Austria. Figure 2 shows the different stages of the powder filling process in an extruder screw shaped capsule using a 3D geometry model. In this model, ~1.6 Mio. particles were filled into the capsule, while pre-consolidation processes such as vibration and tapping were not considered. As shown in Fig. 2 (a) and (b), the particles flowed a long distance from the inserted position to their final location. The fine powder particles rearranged after rebound and concentrated in the region close to the inner side of the screw thread. Particle segregation can be observed after the powder filling process. As the results of particle simulation, the relative density distribution in this extruder screw shaped capsule can be determined and then be mapped in the finite element model, which can be used to simulate the density evolution during the HIP process.

Materials Research Proceedings 38 (2023) 120-130 https://doi.org/10.21741/9781644902837-18

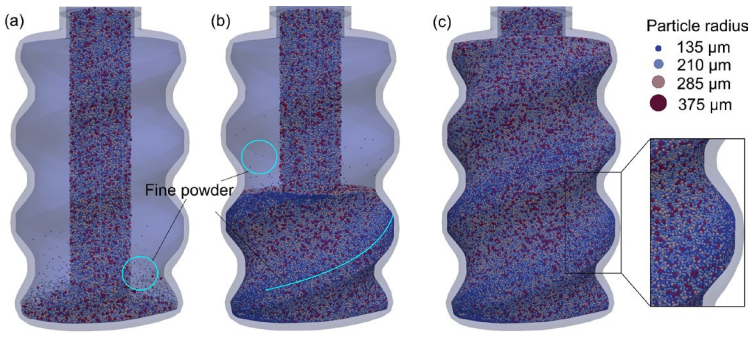

Figure 2: (a) initial, (b) intermediate, and (c) final stages of powder filling in the extruder screw shaped capsule.

Simulation of HIP including the prediction of phase fractions in final component

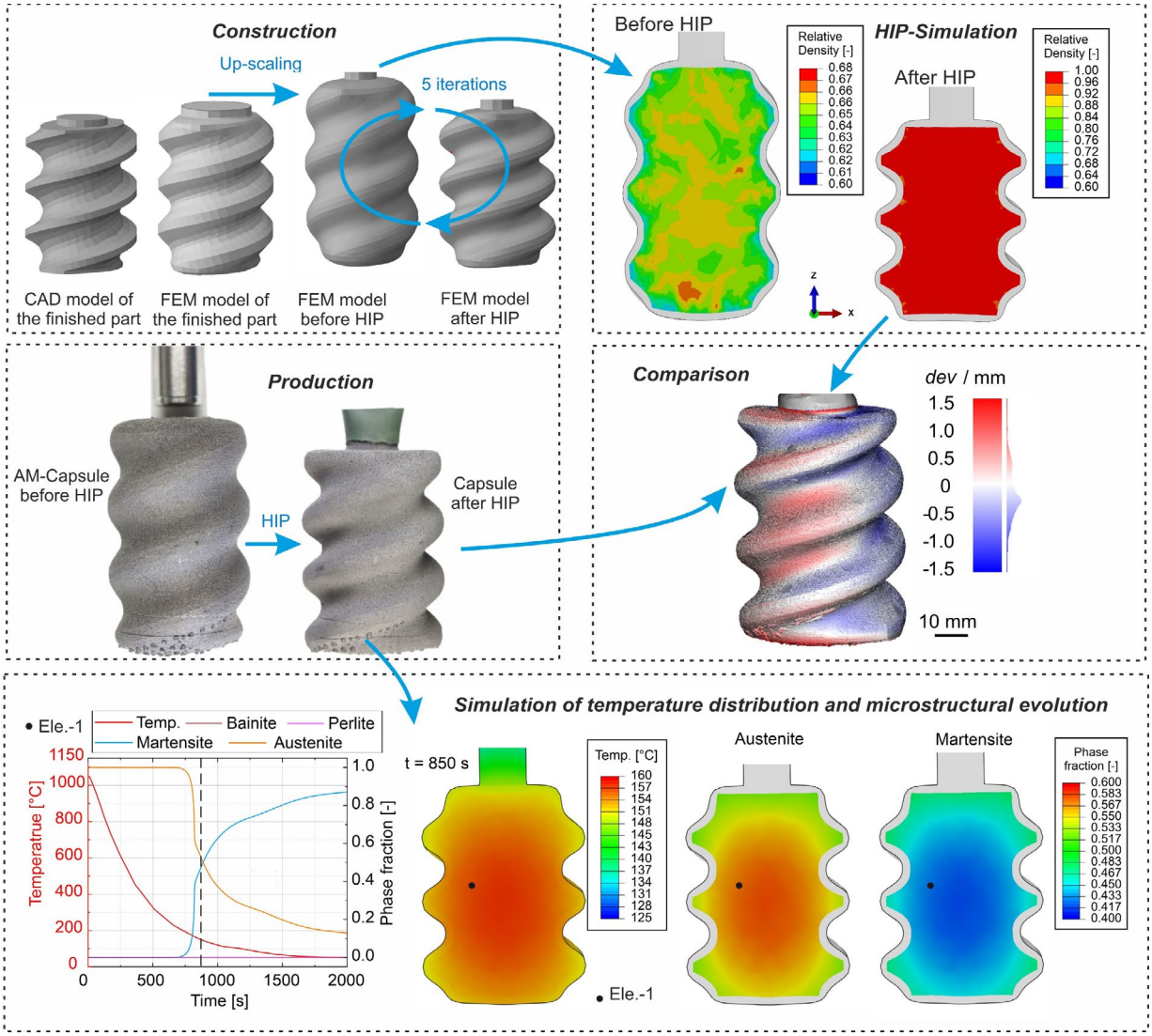

Figure 3: (a) evolution from CAD to optimized capsule geometry and near-net-shape geometry after HIP simulation; (b) relative densities determined in the simulation model prior to HIP (by DEM) and after HIP (by FEM); (c) screw extruder capsule before and after HIP; (d) comparison of optimized capsules for an extruder element in 'as HIP' state; (e) predicted temperature distribution and phase fraction distribution at 850 s.

The HIP densification model based on FEM was implemented beforehand in the user- defined material model (UMAT) [17], which is used to simulate the material in ABAQUS 2020. The required material properties and model parameters were determined experimentally and reported in another publication of the authors [17]. To achieve a near-net-shape component, the modified capsule geometry was generated via "inverse optimization", which was introduced and validated in [12]. To save the computational time, a homogenous powder filling density of 0.62 from tapping tests was assumed for the capsule geometry optimization. Figure 3(a) shows the capsule design steps. As illustrated in Fig. 3(a), the target geometry was first generated based on the CAD-file of the extruder screw element. By adding the capsule region with a thickness of 1.5 mm, the FEM model of the finished part was then generated. Taking this geometry as the target geometry (iteration 1, before HIP), a deformed capsule geometry was obtained after the first simulation step and compared with target geometry. The capsule geometry was adjusted after each iteration and a final shape was predicted after each HIP simulation. After five iterations, the predicted component geometry (iteration 5, after HIP) is identical with the target geometry. The capsule geometry of the last step prior to HIP (iteration 5, before HIP) was used to produce the capsule by Electron Beam Powder Bed Fusion (PBF-EB) (Fig. 3 (c)) on an Arcam A2X machine with pre-heating at 850°C. The build job was conducted with a cross snake scan strategy and a layer thickness of 75 µm, while melting was performed with a line offset of 100 µm and an area energy of about 4 J/mm^2. The large freedom of product geometry as one of the advantages of Additive Manufacturing (AM) methods such as PBF-EB can be utilized if the geometry of the HIP capsule is designed using the aforementioned methods. Benefitting from the capsule design with simulation and production by PBF-EB, the final geometry of complex shaped component after HIP could be assured and the post-processing was expected to be eliminated.

The results shown in Fig. 3 proved the success of this method in achieving near-net-shape production. First, as described in section 3.1 the optimum size and shape for the capsule geometry was determined by FEM simulation. This geometry was used for the powder filling simulation by DEM. Fig. 3(b) shows the predicted powder density distribution after filling and the relative density distribution of the HIP'ed component obtained from the FEM model. From the DEM results, it can be seen that a region with high filling density is presented in the middle of the capsule, whereas the areas close to the inner wall of the screw thread show lower filling densities. The relative densities of the filling powder were between 0.62 and 0.68 with an average value of 0.64, which is 2% higher than the average filling density of 0.62 in a real extruder screw capsule. This 3D density database was imported into the simulation model to simulate the HIP process and obtain the final geometry of the component as well as the density distribution.

Secondly, a capsule of AISI A11 produced by PBF-EB was filled with the powder of AISI L6 and hot isostatically pressed experimentally. After rapid cooling, its final shape (Fig. 3(c)) was measured in 3D with an optical system to obtain the geometrical data file of the outer contour of the real HIP'ed part. By applying the software CloudCompare [18] the differences between the measured geometry and the simulated one were determined automatically and visualized in 3D, as shown in Fig. 3(d). The comparisons in all directions reveal a maximum average deviation of less than 2%.

The simulation of the HIP process was carried out not only using the HIP-model to predict the final geometry (section 2.3) but also the phase transformation model to calculate the microstructural evolution (section 2.4). After densification in the holding stage, the capsule was hardened by quenching directly from the HIP temperature to 100°C within 15 min. Most of the phase transformations that determine the final microstructure take place during the cooling stage, while the prerequisite of modeling phase transformation is the calculation of the spatial temperature distribution through the whole cooling process. As reported in a previous work of the authors [10], the experimentally measured heat transfer coefficients can be defined as thermal

Materials Research Proceedings 38 (2023) 120-130 https://doi.org/10.21741/9781644902837-18

condition to simulate the temperature gradient on the HIP'ed components during cooling. By applying this model, the temperature distribution within the extruder screw was calculated, which allowed the prediction of the phase fraction distributions of bainite, pearlite, martensite, and austenite in the HIP'ed component. Figure 3(e) shows the simulated evolution of the microstructural constituents of a finite element in the center of the HIP'ed part during cooling as well as the temperature distribution within the component and the distribution of the volume fraction of austenite and bainite at a selected time (t=850 s). The final microstructure was predicted to be a mixture of martensite (~87.8%) and retained austenite (~12.2%), which agrees well with the data in the TTT diagram of AISI L6 reported by Eser [14]. This agreement confirms the accuracy of the phase transformation model in calculating the microstructural evolution.

To test the possibility of predicting the precipitate fraction by simulation using the developed phase transformation model, a capsule made of AISI 304 with the geometry (b) shown in Fig. 1 was filled by the powder of AISI 318LN and hot isostatically pressed [10]. Here the duplex stainless steel grade AISI 318LN was selected, as among all intermetallic phases σ–precipitates are the most critical to degrade the mechanical properties of duplex stainless steels. Similar to the previous case study, the densification of the powder, distortion of the capsule, as well as the temperature profile and the precipitation of the σ-phase inside of the being HIP'ed component were calculated in one step. A large temperature gradient up to 4 K/mm, as seen for instance in the temperature distribution at t=215 s in Fig. 4 (a), corresponds well to the distribution of σ–phase volume fraction after cooling (Fig. 4 (b)), despite a rather small predicted average amount of σ-phase of 11 ppm. Although only very limited amount of the σ–phase was precipitated in the simulation due to rapid cooling, its inhomogeneous distribution can still be clearly observed in Fig. 4 (b).

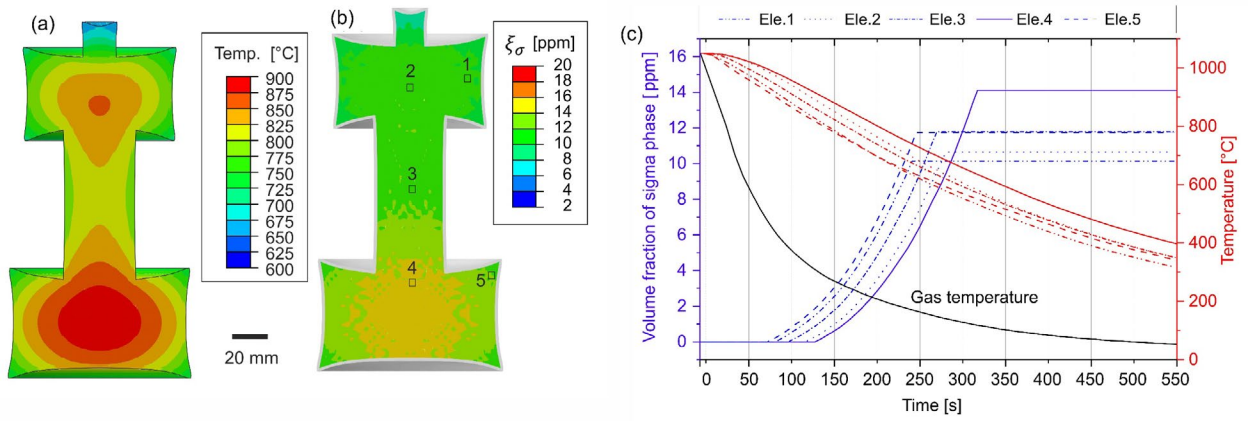

Figure 4: (a) predicted temperature distribution after 215 s; (b) predicted σ–phase distribution at ambient temperature; temperature and predicted σ–phase evolution profiles of five positions 1 -5 marked in (d) in the cooling stage [10].

To further understand the influence of the heat transfer, the predicted evolution of the σ–phase fractions of the five selected elements shown in Fig. 4(b) in the cooling stage were plotted in Fig. 4(c) and analyzed in detail. By observing their positions in the capsule shown in Fig. 4(b), it can be found that the determining factor of their cooling rates is not the shortest distances between them and their respective nearest capsule surface but their distances to the surface in the radial direction. Therefore, the most plausible explanation is that the heat transfer in the capsule depends predominately on the heat flux in the radial direction during rapid cooling.

This demonstrates the significance of a correct consideration of heat transfer in numerical models for the simulation of precipitation in complex shaped components. Moreover, a precisely described temperature distribution is the precondition to understand the anisotropic microstructure of near-net-shape powder HIP components.

Conclusions

In this work, the simulation with a coupled DEM and FEM model was used to calculate the powder density distribution after capsule filling in complex shaped capsules, to predict the capsule shrinkage during the HIP (i.e., the final geometry of the HIP'ed component), and to calculate the evolution of the microstructural constituents in the last rapid cooling stage. All simulation results show good agreements with the experimentally produced products. The main conclusions are summarized in the following.

- In DEM modelling, the particle size distribution was considered as an influencing factor in capsule filling, which leads to a clear visualization of the particle segregation in the filled capsule. The correct predicted powder density distribution will strongly improve the accuracy of the prediction of the capsule shrinkage during HIP simulation.
- Besides the powder density distribution, the optimization of the initial capsule shape is also an essential factor in achieving near-net-shape production of the HIP process. Based on FE-simulations, the capsule of an extruder screw was optimized in this study. Although the optimized capsule geometry is complex and requires precise production, capsules were still successfully produced by AM (PBF-EB), filled with powder and HIP'ed to receive final products.
- A maximum average deviation of less than 2 % was obtained by measuring and comparing the geometries of the simulated and experimentally produced components after HIP. This proves that the implementation of powder density distribution after capsule filling using DEM and capsule geometry optimization using FE-simulation enables near-net-shape production and at the same time combines the respective strengths of AM and HIP.
- In addition, a phase transformation model that was developed to predict the microstructural evolution was also added to the densification model to empower a macroscopic-continuum approach for the simulation of the powder HIP processes. The combined model, which considers different deformation mechanisms during densification and the precipitation or phase transformation kinetics during entire HIP cycle, was successfully implemented as a subroutine in the FE software. The accuracy of it was also confirmed by precisely predicting the shape of the final components and the phase volume distribution therein.
- Furthermore, the application of the simulated temperature distribution in the capsule with the consideration of experimentally determined temperature dependent heat transfer coefficients was proved to be able to further improve the accuracy of the prediction of phase volume fraction, especially for the HIP with integrated rapid cooling.

Acknowledgement

The authors would like to thank Ms. Berenice Kramer at LWT at Ruhr-University Bochum for HIP-cycles, Mr. Markus Mirz at IWM at RWTH Aachen University and Mrs. Marie Franke-Jurisch at Fraunhofer IFAM Dresden for the manufacturing of the extruder screw component. Our appreciation is also to Prof. Dr.-Ing Werner Theisen for valuable discussions.

Funding

This work was performed with the financial support from Germany Research Foundation (DFG) under the project No. 392860940. Thanks also go to the German Federal Ministry for Economic Affairs and Climate Action for financial support of the project IGF-21074 BG. Simulations were

performed with computing resources granted by RWTH Aachen University under project rwth1226.

References

[1] H. V. Atkinson and S. Davies, "Fundamental Aspects of Hot Isostatic Pressing: An Overview," *Metallurgical and Materials Transactions A*, vol. 31A, no. 12, 2000. https://doi.org/10.1007/s11661-000-0078-2

[2] E. Hernández-Nava, P. Mahoney, C. J. Smith, J. Donoghue, I. Todd, and S. Tammas-Williams, "Additive manufacturing titanium components with isotropic or graded properties by hybrid electron beam melting/hot isostatic pressing powder processing," *Scientific Reports*, vol. 9, no. 1, p. 4070, 2019. https://doi.org/10.1038/s41598-019-40722-3

[3] T. Pöschel and T. Schwager, *Computational granular dynamics: Models and algorithms,* 1st ed. Berlin, Heidelberg: Springer, 2010.

[4] P. A. Cundall and O. D. L. Strack, "A discrete numerical model for granular assemblies," *Géotechnique*, vol. 29, no. 1, pp. 47–65, 1979. https://doi.org/10.1680/geot.1979.29.1.47

[5] S. Luding, "Introduction to discrete element methods," *European Journal of Environmental and Civil Engineering*, vol. 12, 7-8, pp. 785–826, 2008. https://doi.org/10.1080/19648189.2008.9693050

[6] A. Bose and W. B. Eisen, *Hot consolidation of powders & particulates*. METAL POWDER INDUSTRIES FEDERATION, 2003.

[7] H. A. Kuhn and C. L. Downey, "DEFORMATION CHARACTERISTICS AND PLASTICITY THEORY OF SINTERED POWDER MATERIALS," *Int. J. Powder Metall.*, vol. 7, no. 1, p. 15, 1971.

[8] M. Abouaf, J. L. Chenot, G. Raisson, and P. Bauduin, "Finite element simulation of hot isostatic pressing of metal powders," *Int. J. Numer. Methods Eng.*, vol. 25, no. 1, pp. 191–212, 1988. https://doi.org/10.1002/nme.1620250116

[9] B. Wikman, A. Svoboda, and H. Å. Häggblad, "A combined material model for numerical simulation of hot isostatic pressing," *Comput. Meth. Appl. Mech. Eng.*, vol. 189, no. 3, pp. 901–913, 2000. https://doi.org/10.1016/S0045-7825(99)00406-5

[10] Y. Deng, J.-L. Zhang, A. Kaletsch, and C. Broeckmann, "Modelling and simulation of densification and σ-phase precipitation in PM duplex steel AISI 318LN during hot isostatic pressing," *Materials Today Communications*, vol. 29, p. 102901, 2021. https://doi.org/10.1016/j.mtcomm.2021.102901

[11] C. van Nguyen, Y. Deng, A. Bezold, and C. Broeckmann, "A combined model to simulate the powder densification and shape changes during hot isostatic pressing," *Computer Methods in Applied Mechanics and Engineering*, vol. 315, pp. 302–315, 2017. https://doi.org/10.1016/j.cma.2016.10.033

[12] S. Riehm *et al.,* "Tailor-made functional composite components using additive manufacturing and hot isostatic pressing," *Powder Metallurgy*, vol. 64, no. 4, pp. 295–307, 2021. https://doi.org/10.1080/00325899.2021.1901398

[13] A. Eser, A. Bezold, C. Broeckmann, I. Schruff, T. Greeb, "Tempering-Simulation of a thick-walled Workpiece made of X40CrMoV5-1 Steel," *Journal of Heat Treatment and Materials*, p. 127.

[14] A. Eser, *Skalenübergreifende Simulation des Anlassens von Werkzeugstahlen*. Dissertation, Aachen, 2014.

[15] M. Avrami, "Kinetics of Phase Change III. Granulation, Phase Change and Microstructure," *Journal of Chemical Physics*, p. 177, 1941. https://doi.org/10.1063/1.1750872

[16] A. Höfter, *Numerische Simulation des Härtens von Stahlbauteilen mit verschleißbeständigen Schichten*. Dissertation, Bochum, 2005. https://doi.org/10.3139/105.100294

[17] C. Broeckmann and T. Weißgärber, *Schlussbericht Maßgeschneiderte verschleißfeste Verbundbauteile durch Additive Manufacturing und heißisostatisches Pressen (Maß-HIP-3D): IGF Vorhaben Nr.: 21074 BG*. Aachen/Dresden, Germany, Herbst, 2022.

[18] D. Girardeau-Montaut, A. Maloney, and R. Janvier, *CloudCompare* (2019).